1. Yaumee Natasha JUSOH[1], 2. Faiz ARITH[2*], 3. Adie MOHD KHAFE[3], 4. Siti Amaniah MOHD CHACHULI[4], 5. Mohd Khanapiah NOR[5], 6. Ahmad Nizamuddin MUSTAFA[6], 7. Fauziyah SALEHUDDIN[7]

Universit Teknikal Malaysia Melaka (1)(2)(3)(4)(7), Imperial College London (6)

doi:10.15199/48.2024.11.17

Carrier Injection Mechanism of Nb-Doped ZnO Thin Films in Light Emission Properties

Abstract. *Hydrothermal growth of Nb-doped ZnO (NZO) films is facilely synthesized as an effective anode buffer layer in enhancing the charge carrier injection, increasing the overall performance of organic light-emitting diodes (OLEDs). The interface between the electrode and the organic layer in an OLED is a critical region that significantly impacts device performance. The presence of an energy barrier at this interface affects charge injection and recombination, influencing brightness, power efficiency, and operational lifetime. Consequently, electrode selection plays a crucial role in determining the overall performance of OLEDs. This study suggests the incorporation of Nb impurity within a ZnO thin film, serving as an interface layer commonly referred to as the anode buffer layer. NZO nanoparticles have also experienced a surface ultraviolet (UV)-ozone treatment and are characterised by UV-visible, SEM, and Raman spectroscopy. SEM images of the NZO films offer insights into the surface morphology of NZO films, while Raman spectroscopy enables the assessment of their structural and compositional attributes. Additionally, analysis by UV-visible spectroscopy demonstrates that the band gap energy of NZO nanoparticles varies with growth time. Measured values for growth times of 8, 10, 12, and 14 hours are 5.09 eV, 4.79 eV, 4.78 eV, and 4.77 eV, respectively. The result revealed that the lowest band gap was achieved by NZO from a 14-hour growth time, thus yielding high recombination and enhancing the carrier injection in the OLED. This study has successfully revealed the potential of UV-ozone-treated NZO ultrathin films, with their enhanced properties, to serve as effective anode buffer materials and improve OLED performance.*

Streszczenie. *Hydrotermiczny wzrost folii ZnO domieszkowanych Nb (NZO) można łatwo syntetyzować jako skuteczną warstwę buforową anody, poprawiającą wtrysk nośnika ładunku, zwiększając ogólną wydajność organicznych diod elektroluminescencyjnych (OLED). Interfejs między elektrodą a warstwą organiczną w OLED to krytyczny obszar, który znacząco wpływa na wydajność urządzenia. Obecność bariery energetycznej na tym interfejsie wpływa na wstrzykiwanie i rekombinację ładunku, wpływając na jasność, wydajność energetyczną i żywotność. W związku z tym wybór elektrod odgrywa kluczową rolę w określaniu ogólnej wydajności diod OLED. Badanie to sugeruje wprowadzenie domieszki Nb do cienkiej warstwy ZnO, służącej jako warstwa pośrednia, powszechnie nazywana warstwą buforową anody. Nanocząsteczki NZO zostały również poddane powierzchniowej obróbce ozonem ultrafioletowym (UV) i charakteryzują się spektroskopią w zakresie widzialnym UV, SEM i Ramana. Obrazy SEM filmów NZO umożliwiają wgląd w morfologię powierzchni filmów NZO, natomiast spektroskopia Ramana umożliwia ocenę ich cech strukturalnych i składu. Ponadto analiza za pomocą spektroskopii widzialnej w zakresie UV pokazuje, że energia pasma wzbronionego nanocząstek N2O zmienia się wraz z czasem wzrostu. Zmierzone wartości dla czasów wzrostu 8, 10, 12 i 14 godzin wynoszą odpowiednio 5,09 eV, 4,79 eV, 4,78 eV i 4,77 eV. Wynik ujawnił, że NZO osiągnęło najniższe pasmo wzbronione w 14-godzinnym czasie wzrostu, zapewniając w ten sposób wysoką rekombinację i usprawniając wtrysk nośnika do OLED. Badanie to z powodzeniem ujawniło potencjał ultracienkich folii NZO poddanych działaniu promieni UV, wraz z ich ulepszonymi właściwościami, jako skuteczne materiały buforowe anodowe i poprawiające wydajność diod OLED. (**Mechanizm wtrysku nośników cienkich warstw ZnO domieszkowanych Nb w właściwościach emisji światła**)*

Keywords: OLEDs, anode buffer layer, bandgap, niobium.
Słowa kluczowe: Diody OLED, warstwa buforowa anody, pasmo wzbronione, niob.

Introduction

Due to their distinctive and fascinating characteristics, organic light-emitting diodes (OLEDs) have become a prominent and widely used display technology [1]. The emergence of OLEDs as a promising display technology is attributed to their various advantages, such as self-luminosity, simplistic structure, ultra-light and thin design, rapid response time, wide viewing angle, low power consumption, and flexible display capabilities [2-11]. Extensive research has been conducted on thin films of indium tin oxide (ITO) due to their distinct properties of transparency and conductivity, making them highly suitable for applications in optoelectronic devices. ITO exhibits a high concentration of free electrons, rendering it a degenerate n-type semiconductor with exceptional electrical conductivity in the range of 2-4 $\times 10^{-4}$ Ω cm. Notably, ITO possesses remarkable transmittance across the visible and near-infrared spectrum, further enhanced by its wide bandgap of 3.3-4.3 eV [12]. Specifically, achieving a precise charge balance is a crucial factor in enhancing the efficiency of OLEDs. Despite the proposals of UV-ozone or oxygen plasma posttreatment, there remains a certain degree of energy barrier at the interface between ITO and organic layers [13]. Hence, by enhancing the injection and transport capabilities of hole carriers, it is possible to attain optimal charge balance outcomes. Incorporating a buffer layer between the ITO and the hole transport layer emerges as a potential approach to tackle this issue. This work aims to enhance charge carrier injection, ultimately improving the OLED device's efficiency [13]. NZO films have potential applications in gas sensing, diluted magnetic semiconduction [14], solar cells [15][16][17][18], and photocatalysis [19].

In recent times, there has been a growing utilisation of metal oxides and metal fluorides as anode buffer layers (ABL) in various applications [13]. These materials have demonstrated enhanced charge injection capabilities at the interface. On top of that, zinc oxide (ZnO) has been reported to possess numerous advantageous qualities, including non-toxicity, exceptional chemical stability, favourable optical transmittance characteristics, and cost-effectiveness. Consequently, it exhibits potential for utilisation in a wide range of optical components [20-22]. ZnO has been increasing interest due to its potential utilisation in various fields, including ultra-violet light emitting and laser devices [22]. Only a limited number of research papers on the preparation of NZO deposited on ITO films exist. Recently, Huang W et al. [13] fabricated ZnO: Nb_2O_5 (NZO) powders using a technique and varied the Nb_2O_5 doping concentrations of 0, 1, and 2 mol%. Powders were produced by sintering metal oxide mixtures at 1273 K for 4 hours in an air environment. The anode in their OLED device configuration was made of an ITO-coated glass substrate with specific dimensions (150 nm thickness, 15 Ω sheet resistance). The NZO layer served as the device's anode buffer layer (ABL), with other layers such as NPB, Alq3, LiF, and Al fulfilling different functions such as hole transport, electron transport/light emission, electron injection, and cathode. Based on the bandgap of ITP/NZO (1%) produces the highest energy bandgap, which is 5.22 eV, where the NZO buffer layer can be attributed to the increase in the anode work function, consequently

reducing the energy barrier for hole injection into the organic layer and improving the injection efficiency [13].

In this research, we utilise ultrathin films of NZO as the ABL and employ a surface modification technique involving UV-ozone treatment. The objective is to optimize the hole injection efficiency of organic light-emitting diodes (OLEDs). The present study focuses on examining the impact of the developed NZO layers on the electrical and optical properties of OLEDs. This investigation is carried out through the utilisation of Scanning Electron Spectroscopy (SEM), Raman Spectroscopy, Ultra-violet (UV-Vis) Spectroscopy, and I-V analysis. The result showed that the band gap of the 14-hour NZO sample is well-matched to the band gap of organic light-emitting materials, ensuring efficient charge transfer and emission processes.

Experimenting procedure

Materials

Zinc acetate, Zn $(CH_3CO_2)_2$ (>=98%), Hexamethylenetetramine, $(CH_2)_6N_4$ (99%), Sodium hydroxide, NaOH (≥ 97.0 %) and Niobium pentoxide, Nb2O5 (99.9%) were purchased from QreC, Scharlab, Merck, Sigma, respectively. All chemicals were used as received without additional purification of reagents was performed.

Preparation of NZO thin film

The ZnO: Nb_2O_5 (NZO) powders were prepared by mixing the ZnO with Nb2O5 doping concentration of 1 mol% under ambient air [21]. Hexamethylenetetramine, $(CH_2)_6N_4$ (99%), and Sodium hydroxide, NaOH (≥ 97.0 %) were added to the mixture to enhance the properties of the NZO powders. An ITO-coated polyethylene terephthalate (PET) film with a sheet resistance of 50 Ω/sq and a thickness of 0.175 mm was employed as the anode buffer layer. Before the hydrothermal deposition of subsequent films, the ITO-coated PET substrate was pretreated with a series of cleaning solutions (ethanol and DI water), dried using a hot plate, and subjected to UV-ozone surface treatment (Osilla L2002A3) for 10 min to preliminarily remove surface impurities [21]. The ultrathin NZO layer was deposited on ITO substrate with different growth hours: 8-hour, 10-hour, 12-hour, and 14-hour, and then followed by being subjected to the UV-ozone treatment for 10 min at room temperature. The emitting area of the device was set to 1.5 × 2.0 cm.

Characterization

A photoelectric measurement system was utilized to measure the current-voltage characteristics of OLED devices [21]. The system consisted of a Keithley-2400 source meter connected to IV-2015 software. The surface morphology of NZO films deposited on the ITO substrate was characterized using SEM measurement with a ZEISS EVO18 instrument [21]. Additionally, the work function variations in NZO films grown at different durations after UV-ozone treatment were assessed via UV-Vis absorbance measurements on a Shimadzu UV-1800 UV/Visible Scanning Spectrophotometer. The investigation concluded with the utilisation of the WITec alpha300 Series Raman Spectroscopy method to analyse the vibrational modes and molecular structure of the materials. All experiments in this study were conducted with multiple repetitions to ensure data reliability.

Result and discussion

SEM analysis

The surface morphologies of NZO thin films with a 1 mol% Nb dopant concentration, deposited on ITO substrates for varying growth durations (8, 10, 12, and 14 hours), were investigated using scanning electron microscopy (SEM), as illustrated in Figure 1. The presented SEM images reveal that incorporating 1% Nb into the NZO matrix leads to the emergence and proliferation of nanoparticles on the film surface. This finding was similar to that reported in Ref. [24]. The grain shape can be distinguishable for 8-hour, 10-hour, 12-hour, and 14-hour NZO thin films. It can be observed that the grain size increased as the NZO growth hours increased. Following exposure for 8 and 10 hours, a slight decline in the clarity of the grains was observed. The 8-hour sample shows small aggregates of atoms, which means that at this stage, the atoms are not yet fully formed into nanoparticles and are still in the process of aggregating together. The 10-hour and 12-hour samples show the formation of nanoparticles. However, these nanoparticles are not as dense or well-defined as the nanoparticles in the 14-hour sample. Spherical grains were observed through NZO thin films with 1% of Nb for 14 hours, as shown in Fig. 1(d). The SEM image indicates an improvement in the film crystallinity, similar to Ref. [25]. The nanoparticles in the 14-hour sample exhibit higher density and better definition compared to the nanoparticles in the 10-hour and 12-hour samples. The diameter of the nanoparticles in the 14-hour sample is reported to be around 32.19 nm, which is slightly smaller than the diameter reported by Hammad et al., which is 35.77 nm [29]. Nevertheless, the presence of Nb had a positive effect on enhancing the surface smoothness of ZnO. Conversely, small nanospheres were detected alongside the ZnO grains in all Nb-doped samples. This observation suggests that metallic nanospheres composed of Nb were uniformly distributed within the ZnO lattice structure [25].

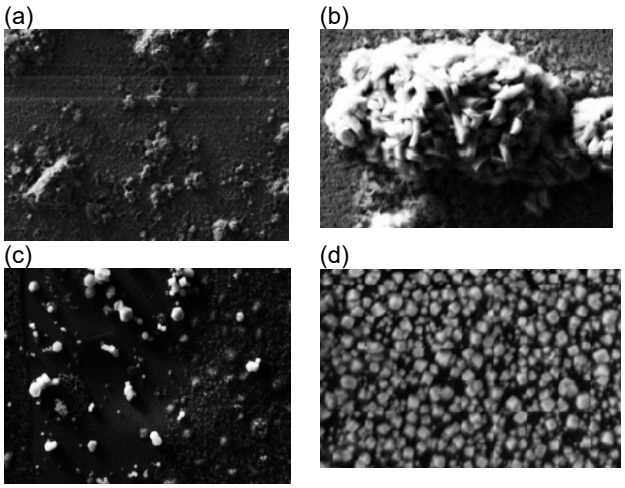

Fig.1. Scanning electron microscope (SEM) images of the 1% Nb sample at various growth durations: (a) 8 hours, (b) 10 hours, (c) 12 hours, and (d) 14 hours.

Raman spectroscopy

The deviation from the commonly reported Raman peak positions of 685 cm^{-1} for Nb_2O_5 and 437 cm^{-1} for ZnO, resulting in peak positions of 635 cm^{-1} and 400 cm^{-1} [2][27], can be attributed to various factors, including sample characteristics, experimental conditions, and instrument calibration. The characteristic frequency of the E2 mode of ZnO in the Raman spectrum is around 437 cm^{-1}, indicating the vibration of oxygen atoms around zinc atoms in the crystal lattice [31][32]. The strong intensity of the ZnO peak in the Raman spectrum indicated a high degree of crystallinity in the ZnO film. Conversely, a sharper and more intense peak would further suggest a significantly higher degree of crystallinity. The presence of the ZnO peak in the

Raman spectrum provides evidence for the wurtzite crystal structure of the ZnO film, which is the most stable structure for ZnO. The Raman spectrum of the image in Fig. 2. shows a peak at around 635 cm^{-1}, corresponding to the characteristic frequency of the A1g mode of Nb in the Nb-doped ZnO film. The intensity of the Nb peak in the Raman spectrum indicates the 1% mol concentration of Nb dopants in the ZnO film. The existence of the Nb peak in the Raman spectrum provides compelling evidence for the successful incorporation of Nb dopants into the ZnO crystal lattice. This observation is attributable to the fact that the A1g mode, identified in the spectrum, specifically corresponds to the vibrational signature of niobium atoms within the Nb crystal lattice.

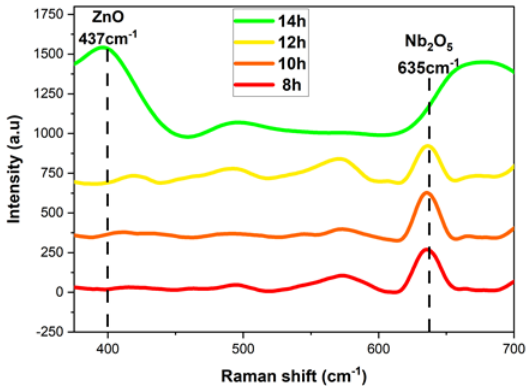

Fig.2. Raman spectra of the NZO with different time growth.

UV-Vis spectroscopy

The transmittance spectra of the thin films were analyzed using UV-vis spectroscopy, which measures the amount of light that passes through a material. ZnO is known to have high transmittance in the UV region, with a transmittance of over 90% in the range of 300-400 nm [33][34]. The transmittance of all four samples is lower than the transmittance of ZnO in the visible region (400-800 nm). This is possibly due to the existence of Nb in the samples, which may absorb some of the visible light. The presence of Nb dopants in the samples can lead to the absorption of some visible light, resulting in lower transmittance in the visible region. Typically, the addition of Nb dopants in ZnO can create energy levels within the bandgap, resulting in the absorption of photons in the visible spectrum. Electrons are excited from the valence band to dopant-induced energy levels within the bandgap, and then undergo transitions to the conduction band, as part of the visible light absorption mechanism in Nb-doped materials. The presence of Nb dopants creates energy states within the bandgap of ZnO, inducing absorption of visible light and thus attenuating overall transmittance. This effect leads to lower transmittance values compared to pristine ZnO. The transmittance of the samples increases with increasing wavelength. This is because the photon energy is lower at a longer wavelength and, hence, less likely to be absorbed by the Nb dopants. The energy of photons at longer wavelengths is lower, making them less likely to be absorbed by the Nb dopants, resulting in increased transmittance.

The lower transmittance of the 14-hour sample in the visible region (400-800 nm) compared to the 8-hour sample can be attributed to the higher absorption of visible light by the Nb dopants in the 14-hour sample. The inclusion of Nb dopants within the sample induces the absorption of visible light, particularly in the shorter wavelength range. This phenomenon consequently causes a reduction in transmittance across the visible spectrum. The absorption behavior of Nb dopants is more prominent in the visible spectrum, causing a decrease in transmittance in this wavelength range. The 14-hour sample, which has been exposed to Nb dopants for a longer duration, may have a higher concentration of dopants, leading to increased absorption of visible light and lower transmittance in the visible region compared to the 8-hour sample.

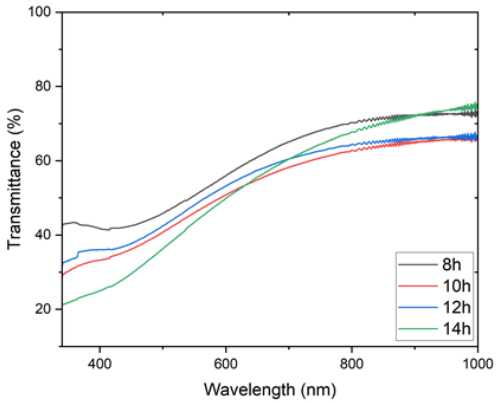

Fig.3. The visible light transmittance through the proposed OLEDs structure.

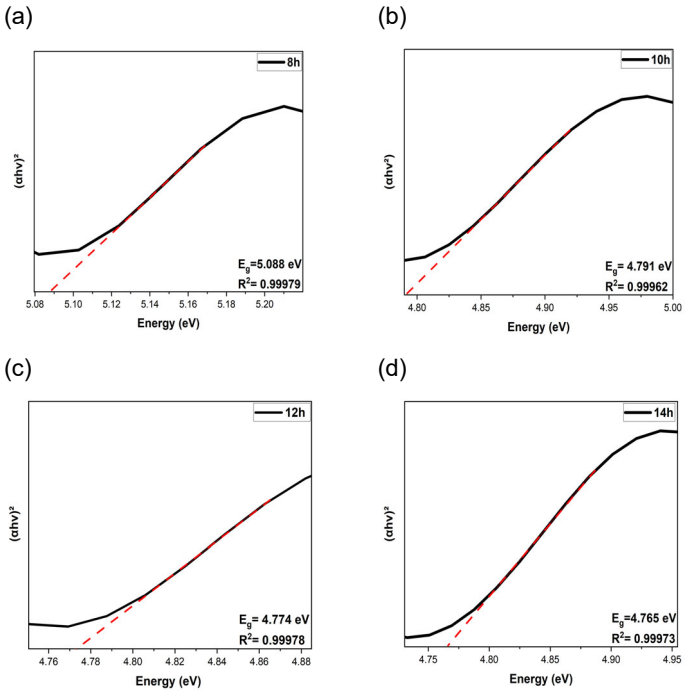

Fig.4. Band gap of Nb_2O_5 doped ZnO on ITO substrate with different time growth (a) 8-hour (b) 10-hour (c) 12-hour (d) 14-hour.

Table 1: Band gap of NZO on ITO substrate with different time growth.

Growth Hour	Energy Gap, Eg (eV)
8	5.09
10	4.79
12	4.78
14	4.77

The incorporation of metallic niobium into the ZnO crystal structure leads to a notable increase in band gap energy. The embedding of Nb dopant in the ZnO lattice leads to structural changes and an increase in the structural disorder in the ZnO lattice [28]. The conducted study determined that the most favourable duration for the growth of Nb-doped ZnO films while maintaining a consistent

concentration is 8 hours, based on Figure 4. This is the growth duration that yields the maximum bandgap. The films that underwent an 8-hour growth period exhibited the highest degree of crystallinity and the lowest density of defects. It is postulated that these factors are accountable for the elevated bandgap. The bandgap regression value is approximately 1, indicating the perfect extrapolation.

The main difference between the 8-hour and 14-hour ZnO films based on Table 1 in terms of band gap is that the 14-hour film has a slightly lower band gap. The 14-hour film is more crystalline than the 8-hour film, resulting in a lower band gap and more freely moving electrons. The increased crystallinity in the 14-hour film allows for better electron mobility, resulting in a slightly lower band gap than the 8-hour film. The band gap of the 14-hour ZnO sample (4.77 eV) was 6% lower than the band gap of the 8-hour ZnO sample (5.09 eV). This decrease in band gap with growth hour is likely due to the increased crystallinity of the 14-hour ZnO film.

Conclusion

The study showcases the successful utilisation of NZO thin films on flexible ITO substrates using a low-temperature technique. The aforementioned accomplishment enables the incorporation of ZnO-derived materials into flexible electronic devices while preserving the inherent stability of the underlying structure. The 14-hour ZnO sample has a dense and well-defined morphology, indicating a high-quality film structure. It demonstrates high transmittance in the visible region, which is crucial for efficient light emission in OLED devices. The band gap of the 14-hour ZnO sample is well-matched to the band gap of organic light-emitting materials, ensuring efficient charge transfer and emission processes. These properties collectively suggest that the 14-hour ZnO sample can effectively serve as an anode buffer layer in OLED devices, providing both electrical conductivity and optical transparency for improved device performance. Overall, OLEDs have revolutionized the display industry and continue to be an area of active research and development [29][34].

Acknowledgement

This work was supported by Universiti Teknikal Malaysia, Melaka, Malaysia.

Authors

Yaumee Natasha Jusoh, Universiti Teknikal Malaysia Melaka, Faculty of Electronics and Computer Technology Hang Tuah Jaya E-mail: M122310001@student.utem.edu.my

Faiz Arith, Universiti Teknikal Malaysia Melaka, Faculty of Electronics and Computer Technology Hang Tuah Jaya E-mail: faiz.arith@utem.edu.my

Adie Mohd Khafe, Universiti Teknikal Malaysia Melaka, Faculty of Electronics and Computer Technology Hang Tuah Jaya E-mail: adie@utem.edu.my

Siti Amaniah Mohd Chachuli, Universiti Teknikal Malaysia Melaka, Faculty of Electronics and Computer Technology Hang Tuah Jaya E-mail: sitiamaniah@utem.edu.my

Mohd Khanapiah Nor, Universiti Teknikal Malaysia Melaka, Faculty of Electronics and Computer Technology Hang Tuah Jaya E-mail: khanapiah@utem.edu.my

Ahmad Nizamuddin Mustafa, Department of Materials, Faculty of Engineering, Imperial College London, E-mail: a.bin-muhammad-mustafa21@imperial.ac.uk

Fauziyah Salehuddin, Universiti Teknikal Malaysia Melaka, Faculty of Electronics and Computer Technology Hang Tuah Jaya E-mail: fauziyah@utem.edu.my

REFERENCES

[1] Mullemwar, S. Y., Kalyani, N. T., & Dhoble, S. J. (2023). OLEDs: Emerging technology trends and designs. In Phosphor Handbook (pp. 307-328). Woodhead Publishing.

[2] Burrows, P. E., Gu, G., Forrest, S. R., Vicenzi, E. P., & Zhou, T. X. (2000). Semitransparent cathodes for organic light emitting devices. *Journal of Applied Physics*, *87*(6), 3080-3085.

[3] Hung, L. S., Tang, C. W., & Mason, M. G. (1997). Enhanced electron injection in organic electroluminescence devices using an Al/LiF electrode. *Applied Physics Letters*, *70*(2), 152-154.

[4] Mason, M. G., Hung, L. S., Tang, C. W., Lee, S. T., Wong, K. W., & Wang, M. (1999). Characterization of treated indium–tin–oxide surfaces used in electroluminescent devices. *Journal of Applied Physics*, *86*(3), 1688-1692.

[5] Kim, H., Pique, A., Horwitz, J. S., Mattoussi, H., Murata, H., Kafafi, Z. H., & Chrisey, D. B. (1999). Indium tin oxide thin films for organic light-emitting devices. *Applied physics letters*, *74*(23), 3444-3446.

[6] Yu, H. Y., Feng, X. D., Grozea, D., Lu, Z. H., Sodhi, R. N. S., Hor, A. M., & Aziz, H. (2001). Surface electronic structure of plasma-treated indium tin oxides. *Applied Physics Letters*, *78*(17), 2595-2597.

[7] Hu, T., Zhang, F., Xu, Z., Zhao, S., Yue, X., & Yuan, G. (2009). Effect of UV–ozone treatment on ITO and post-annealing on the performance of organic solar cells. *Synthetic Metals*, *159*(7-8), 754-756.

[8] Li, C. N., Kwong, C. Y., Djurišić, A. B., Lai, P. T., Chui, P. C., Chan, W. K., & Liu, S. Y. (2005). Improved performance of OLEDs with ITO surface treatments. *Thin Solid Films*, *477*(1-2), 57-62.

[9] Ma, K. X., Ho, C. H., Zhu, F., & Chung, T. S. (2000). Investigation of surface energy for organic light emitting polymers and indium tin oxide. *Thin Solid Films*, *371*(1-2), 140-147.

[10] Rudawska, A., & Jacniacka, E. (2009). Analysis for determining surface free energy uncertainty by the Owen–Wendt method. *International journal of adhesion and adhesives*, *29*(4), 451-457.

[11] Wu, C. C., Wu, C. I., Sturm, J. C., & Kahn, A. (1997). Surface modification of indium tin oxide by plasma treatment: An effective method to improve the efficiency, brightness, and reliability of organic light emitting devices. *Applied Physics Letters*, *70*(11), 1348-1350.

[12] Kim, H., Pique, A., Horwitz, J. S., Mattoussi, H., Murata, H., Kafafi, Z. H., & Chrisey, D. B. (1999). Indium tin oxide thin films for organic light-emitting devices. *Applied physics letters*, *74*(23), 3444-3446.

[13] Huang, W. L., Chu, S. Y., & Kao, P. C. (2022). Investigation of improving organic light-emitting diodes efficiency using an ultra-thin ultraviolet-ozone-treated Nb-doped ZnO film as anode buffer layer. *Journal of Alloys and Compounds*, *921*, 166033.

[14] Satheesan, M. K., Vani, K., & Kumar, V. (2017). Acceptor-defect mediated room temperature ferromagnetism in (Mn2+, Nb5+) co-doped ZnO nanoparticles. *Ceramics International*, *43*(11), 8098-8102.

[15] Aliyaselvam, O. V., Junos, S. M., Arith, F., Izlan, N., Said, M. M., & Mustafa, A. N. (2022). Optimization of Copper (I) Thiocyanate as Hole Transport Material for Solar Cell by Scaps-1D Numerical Analysis. *Przegl*.

[16] Aliyaselvam, O. V., Arith, F., Mustafa, A. N., Chelvanathan, P., Azam, M. A., & Amin, N. (2023). Incorporation of green solvent for low thermal budget flower-like Copper (I) Iodide (γ-CuI) for high-efficiency solar cell. *Journal of Materials Science: Materials in Electronics*, *34*(16), 1274.

[17] Noorasid, N. S., Arith, F., Mustafa, A. N., Azam, M. A., Suhaimy, S. H. M., & AL-ANI, O. A. (2021). Effect of Low Temperature Annealing on Anatase TiO2 Layer as Photoanode for Dye-Sensitized Solar Cell. *Przeglad Elektrotechniczny*, *97*(10).

[18] Jafari, H., Sadeghzadeh, S., Rabbani, M., & Rahimi, R. (2018). Effect of Nb on the structural, optical and photocatalytic properties of Al-doped ZnO thin films fabricated by the sol-gel method. *Ceramics International*, *44*(16), 20170-20177.

[19] Keis, K., Magnusson, E., Lindström, H., Lindquist, S. E., & Hagfeldt, A. (2002). A 5% efficient photoelectrochemical solar cell based on nanostructured ZnO electrodes. *Solar energy materials and solar cells*, *73*(1), 51-58.

[20] Liang, S., Sheng, H., Liu, Y., Huo, Z., Lu, Y., & Shen, H. J. J. O. C. G. (2001). ZnO Schottky ultraviolet photodetectors. *Journal of crystal Growth*, *225*(2-4), 110-113.

[21] Rensmo, H., Keis, K., Lindström, H., Södergren, S., Solbrand, A., Hagfeldt, A., ... & Muhammed, M. (1997). High light-to-

energy conversion efficiencies for solar cells based on nanostructured ZnO electrodes. *The Journal of Physical Chemistry B*, *101*(14), 2598-2601.
[22] Dong, L., Jiao, J., Tuggle, D. W., Petty, J. M., Elliff, S. A., & Coulter, M. (2003). ZnO nanowires formed on tungsten substrates and their electron field emission properties. *Applied Physics Letters*, *82*(7), 1096-1098.
[23] Taziwa, R., Ntozakhe, L., & Meyer, E. (2017). Structural, morphological and Raman scattering studies of carbon doped ZnO nanoparticles fabricated by PSP technique. *J Nanoscience & Nanotechnology Res*, *1*, 1-3.
[24] Cao, C., Ford, D., Bishnoi, S., Proslier, T., Albee, B., Hommerding, E., ... & Zasadzinski, J. F. (2013). Detection of surface carbon and hydrocarbons in hot spot regions of niobium superconducting rf cavities by Raman spectroscopy. *Physical Review Special Topics-Accelerators and Beams*, *16*(6), 064701.
[25] Zhang, H., Deng, J., Pan, Z., Bai, Z., Kong, L., & Wang, J. (2017). Structural and optical properties of Nb-doped β-Ga2O3 thin films deposited by RF magnetron sputtering. *Vacuum*, *146*, 93-96.
[26] Wang, Z. L. (2004). Zinc oxide nanostructures: growth, properties and applications. *Journal of physics: condensed matter*, *16*(25), R829.
[27] Hung, L. S., Tang, C. W., & Mason, M. G. (1997). Enhanced electron injection in organic electroluminescence devices using an Al/LiF electrode. *Applied Physics Letters*, *70*(2), 152-154.
[28] Mertens, K. (2018). Photovoltaics: fundamentals, technology, and practice. John Wiley & Sons.
[29] Hammad, A. H., & Abdel-wahab, M. S. (2021). Characterization of niobium-doped zinc oxide thin films: Structural changes and optical properties. *Materials Today Communications*, *26*, 101791.
[30] Peach, L. A. (1997). Optical filters select appropriate wavelengths. *Laser focus world*, *33*(2), 141-150.
[31] Milošević, I., Stevanović, V., Tronc, P., & Damnjanović, M. (2006). Symmetry of zinc oxide nanostructures. *Journal of Physics: Condensed matter*, *18*(6), 1939.
[32] Hirata, Y. (2020). Unified representation of thermal conductivities for movement of electrons and lattice vibration of atoms. *Ceramics International*, *46*(8), 10130-10134.
[33] Alias, N. S. N. M., Arith, F., Mustafa, A. N., Ismail, M. M., Azmi, N. F., & Saidon, M. S. (2022). Impact of Al on ZnO Electron Transport Layer in Perovskite Solar Cells. *Journal of Engineering & Technological Sciences*, *54*(4).
[34] Alias, N. S. N. M., Arith, F., Mustafa, A. N. M., Ismail, M. M., Chachuli, S. A. M., & Shah, A. S. M. (2022). Compatibility of Al-doped ZnO electron transport layer with various HTLs and absorbers in perovskite solar cells. *Applied Optics*, *61*(15), 4535-4542.